Chapter 4

Entanglement entropies across dynamical quantum phase transitions: From skyrmionic to ferromagnetic phases

4.1 Introduction

Quantum mechanics is a fundamental theory that underpins our understanding of matter and energy at the microscopic scale. In recent years, the study of the dynamical properties of quantum systems has emerged as a central theme in this field [87, 88].

Quantum systems are inherently dynamic, with their properties and behavior evolving over time in complex and often unpredictable ways. Understanding these dynamics is essential for advancing cutting-edge technologies, including quantum computing, quantum communication, and quantum sensing. Moreover, studying dynamical properties provides

deeper insights into the fundamental nature of quantum systems, shedding light on the principles that govern their evolution.

One of the most intriguing and useful concepts in quantum mechanics is entanglement, where two or more quantum systems become correlated in such a way that their behavior becomes inseparable. Entanglement is a critical resource for quantum technologies, such as quantum cryptography, and its study is essential for the development of the field.

Recent experimental advances have enabled researchers to study the dynamics of quantum systems in real-time. For example, ultra-cold atoms in optical lattices and trapped ions are some of the systems where real-time dynamical phenomena have been observed. Furthermore, experiments utilizing THz pulses in solids [89, 90, 91, 92] and high magnetic field pulse experiments [93] have provided valuable insights into the dynamical properties of corresponding quantum systems.

Skyrmions, a class of topological solitons, have garnered significant interest as promising topological materials owing to their unique non-collinear spin textures[116, 117, 118, 169, 170, 171]. Despite their small size, their non-trivial topological characteristics give them a remarkable degree of thermal stability even at room temperature. Skyrmions are considered strong candidates for information carriers in next-generation spintronic devices owing to these properties[119, 179, 180]. A skyrmion can be described as a nonlinear localized mode with a stable shape. Although magnetic skyrmions have been studied classically with great success over the past fifty years, the nanoscale of skyrmions has made it important to study their quantum properties[138, 222, 223, 224], thus this is one of the highly investigated topics in current literature[193, 194, 195, 199, 202, 203, 225, 226, 227, 228, 229, 230, 231, 232, 233, 234, 235, 236]. One of the recent studies conducted by Sotnikov et al. identified the skyrmion phase in the ground state of a triangular spin lattice with nearest-neighbor Heisenberg anti-ferromagnetic coupling and Dzyaloshinskii-Moria interactions by observing quantum scalar chirality [109]. They used scalar chirality as an

analogous to classical topological charge to justify their report. However, it was found that the scalar chirality fails to distinguish the Helical phase and skyrmion with absolute precision. This is because the skyrmion phase is not orthogonal to the helical phase, resulting in a smooth transition between both unless a topologically exclusive quantifier is sought. Siegl et al. used quantities, such as winding parameter and topological index to identify the topological phase and trivial phase [237]. Despite these progresses, a definitive way to fully quantify the quantum skyrmion is still lacking, and studies are ongoing to address this problem.

In a previous study by our group, we demonstrated the occurrence of a robust dynamical quantum phase transition (DQPT) when the system underwent a rapid quench from a topological (skyrmionic) phase to a ferromagnetic phase[238]. Here, we considered a system described by a Hamiltonian incorporating the Zeeman energy of the applied field, ferromagnetic nearest-neighbor Heisenberg exchange interaction, antiferromagnetic next-nearest-neighbor Heisenberg exchange interaction, and anisotropic Dzyaloshinskii-Moriya interaction (DMI). Moreover, a certain system has demonstrated enhanced entanglement entropy around critical points of DQPTs [95]. The robustness of entanglement properties in the topological skyrmionic phase, along with the enhanced entanglement entropy around DQPTs, underscores the importance of studying the entanglement characteristics of topological skyrmions. This research explores how DQPTs influence entanglement entropy and related observables in a skyrmionic system. To achieve this, we analyzed the dynamical behavior of various observables in the presence and absence of DQPTs. The system was initially prepared in a skyrmion phase and subjected to a rapid quench, driving it into a ferromagnetic or helical state through unitary evolution. We then systematically tracked and quantified changes in the relevant quantities throughout the transition process.

The subsequent sections of this paper are organized as follows: Section 4.2 outlines the model Hamiltonian and lattice that were utilized. In this section, we introduce the physical

observables and methods that were employed for our analysis. Section 4.3 presents our findings and briefly elucidates the main features of the results compared with the literature. This is followed by Section 4.4, where we discuss the implications of the results on the theoretical model.

4.2 Model and methods

4.2.1 Spin model

In this study, we examine a two-dimensional quantum spin-1/2 system located on a triangular lattice and utilize a circular boundary to account for the skyrmion geometry (19 spin configuration shown in Fig. C.1). A periodic boundary condition is used to reduce the boundary effects.

The Hamiltonian of the system is given by:

$$\hat{H} = B\sum_i \hat{\mathbf{S}}_i^z + J_1 \sum_{\langle i,j\rangle} \hat{\mathbf{S}}_i\hat{\mathbf{S}}_j + \quad J_2 \sum_{\langle\langle i,j\rangle\rangle} \hat{\mathbf{S}}_i\hat{\mathbf{S}}_j + \sum_{i<j} \mathbf{D}_{i,j}\left[\hat{\mathbf{S}}_i \times \hat{\mathbf{S}}_j\right], \tag{4.1}$$

In order to achieve a noncollinear spin texture and helical phases, we utilize a combination of competing interactions, including those between nearest and next nearest neighbors, denoted as J_1 and J_2, respectively, as well as the Dzyloshinskii-Moria interaction. The DMI vector is perpendicular to the bonds that connect sites i and j. For a triangular lattice, three lattice vectors exist, and the orientation of the DMI vector is determined by the orientation of the lattice vectors. Assuming that $\mathbf{a_{ij}}$ represents a unit vector along the lattice vector, the direction of the DMI will align with $\mathbf{a_{ij}} \times \hat{z}$. A similar Hamiltonian and model were previously considered in [109].

4.2.2 Dynamical quantum phase transition

Instead of the conventional temperature T, considering a complex temperature, denoted as z, the partition function can be denoted as, $Z(z)$. When the zeros of this partition function coincide with the real axis, it leads to non-analyticities in the corresponding free energy [96, 99]. Consider the quantity known as the Loschmidt amplitude, as expressed in Eq. 4.2:

$$\mathscr{G}(t) = \langle \psi_0 | e^{-i\hat{H}(\lambda)t} | \psi_0 \rangle. \tag{4.2}$$

Here $|\psi_0\rangle$ is the ground state of the system Hamiltonian $\hat{H}(\lambda_0)$ with parameter λ_0 and $e^{-i\hat{H}(\lambda)t}|\psi_0\rangle$ is the evolved state under the influence of a Hamiltonian $\hat{H}(\lambda)$ for a duration of time t. Where the parameter λ_0 of the Hamitoian is quenched to λ at $t = 0$. Here $e^{-i\hat{H}(\lambda)t}$ is the unitary evolution operator with the parameter λ in the Hamiltonian. This expression is akin to the partition function in thermodynamic equilibrium, where $Z = \mathrm{Tr}(e^{-\beta\hat{H}})$, but with a twist—here, instead of temperature, we have a complex temperature denoted as it. In this context, $\hat{H}$ represents the Hamiltonian, and β is the inverse temperature. The function $\mathscr{G}(t)$ serves a similar role as the partition function of complex temperature. Consequently, we can define a corresponding free energy, as shown in Eq. 4.3:

$$\mathscr{L}(t) = -\lim_{N\to\infty} \frac{1}{N} \ln |\mathscr{G}(t)|^2. \tag{4.3}$$

This is known as the rate function of the return probability or simply the rate function. The zeros of the Loschmidt amplitude induce non-analyticities in the rate function, serving as the signature of a DQPT.

4.2.3 Quantum scalar chirality

The scalar chirality is regarded as the quantum counterpart of the topological invariant that serves to differentiate the skyrmion (topological) phase from other phases of the system,

as outlined in [109].

$$\mathbf{C}_{\Psi} = \frac{L}{\pi} \left\langle \hat{S}_1 \left[\hat{S}_2 \times \hat{S}_3 \right] \right\rangle . \tag{4.4}$$

Here, L refers to the number of non-overlapping elementary triangular patches that cover the lattice, with each patch comprising three adjacent spins. The scalar chirality of any one of such patches is identical owing to the translational and rotational symmetries of the lattice. In the classical limit, this quantity is equivalent to the topological invariant that distinguishes a magnetic skyrmion[109].

4.2.4 Entanglement entropy

The entropy of entanglement, or entanglement entropy (EE), quantifies the level of entanglement between two composite subsystems of a given system. In this context, the larger system can be partitioned into subsystems A and its complement, $\tilde{A}$. The composite Hilbert space H_S of the system is formed by the tensor product of the local Hilbert spaces H_A and $H_{\tilde{A}}$. The entanglement entropy is then computed by considering the reduced density matrix of subsystem A, denoted as ρ_A, and evaluating the von-Neumann entropy.

$$\mathscr{S}_A = -tr(\rho_A \log(\rho_A)) \tag{4.5}$$

A non-zero value of $\mathscr{S}_A$ indicates the presence of entanglement between the two subsystems. The magnitude of the entanglement entropy reflects the degree of entanglement between the subsystems, where a larger value corresponds to a stronger degree of entanglement. For the purpose of this study, we considered a 19-spin system, out of which subsystem A consists of 9 spins (see Fig. C.1 in appendix C-I).

4.2.5 Topological entanglement entropy

The topological entanglement entropy (TEE), denoted as $\mathscr{S}_{topo}$, is a universal measure of many-particle quantum entanglement in the ground state of a topologically ordered two-dimensional system with a mass gap [84, 85]. In bipartite entanglement entropy or entanglement entropy, the extent of entanglement between a partition and its complementary (remaining part of the system) is measured. The entanglement entropy follows an "area law", where it is proportional to the area of the boundary between the two partitions. Kitaev and Preskill [84] and Levin and Wen [85] independently showed that besides the area-dependent term, the entanglement entropy has a part that solely depends on the topology of the boundary curve. This term is known as topological entanglement entropy (TEE).

The TEE is defined by considering three partitions of the system plane P, Q and R and the remaining part of the system, on which P, Q and R are embedded, is labeled as S (see Fig. C.2 in appendix C-I). $\mathscr{S}_P$ denotes the entanglement entropy of the reduced density matrix ρ_P of subsystem P, $\mathscr{S}_{P\cup Q}$ is the entropy of the subsystem $P \cup Q$ with reduced density matrix $\rho_{P\cup Q}$, and so on. Here, $\cup$ denotes the set operation union. The TEE, $\mathscr{S}_{topo}$, is then defined using the partitions P, Q and R as follows:

$$\mathscr{S}_{topo} = \mathscr{S}_P + \mathscr{S}_Q + \mathscr{S}_R - \mathscr{S}_{P\cup Q} - \mathscr{S}_{Q\cup R} - \mathscr{S}_{P\cup R} + \mathscr{S}_{P\cup Q\cup R} \tag{4.6}$$

For a large system, $\mathscr{S}_{topo}$ is defined to be invariant under smooth deformations of the Hamiltonian and will only change when a quantum critical point is encountered.

4.3 Results and discussion

After performing quenches from the skyrmionic phase to helical or ferromagnetic phase, we studied the dynamical behavior of several quantities. The initial state of the system was

a skyrmion ground state defined by the parameters $D = 1,;J_1 = -0.5D,;J2 = 0.1D$, and $B = 0.85D$. Our main focus was on the change in entropy and related quantities.

Fig.4.1 (a) the entropy, after a quench from the skyrmion to the ferromagnetic phase, $\mathscr{S}_A$, was measured for a long duration and an increase in entropy was observed. Subsequently, the system relaxed to a finite entropy value. Similarly, the entropy was measured for a skyrmion to helical quench and an increase in entropy was observed (Fig.4.1 (b)). Here, the system subsequently relaxed to a finite value as well, similar to the quench from the skyrmionic to ferromagnetic phase. Based on the results shown in Figs.4.1 (a) and (b), specifically, we observe a rise in entropy during both quench protocols, irrespective of the presence of DQPT. We did not observe an enhanced entropy around the critical points of DQPT, as reported by Ref.[95]. This suggests that the primary driver of entanglement growth in this system is not the DQPT itself, but rather the inherent non-equilibrium nature of the quench process. This observation aligns with the fundamental principle of the second law of thermodynamics: entropy, a measure of disorder, tends to increase in closed systems.

The overlap between the states undergoing quenches from skyrmionic to ferromagnetic/helical phase can be defined using Wootters' distance [239] given by

$$w_d(|\psi_i\rangle, |\psi_f\rangle) = \cos^{-1} |\langle\psi_i|\psi_f\rangle|. \tag{4.7}$$

We have shown the Wootters' distance in Fig.4.1 (c). As time progresses, the Wootters' distance reaches its maximum, indicating the orthogonality of the evolved states, and the identical relaxation of entropies in Fig.4.1 (a) and Fig. 4.1 (b) is not owing to the states following the same path during their quenches. Fundamentally, the quench operation is a unitary process, meaning that it preserves the quantum coherence of the system and is inherently time-reversible. This implies that, principally, the evolution of the system can

be retraced by applying the inverse quench, allowing it to return to its initial state without loss of information.

Next, we compared the rate function with the rate of change of entanglement entropy, $\frac{d\mathscr{S}}{dt}$, where $\mathscr{S}$ represents the von Neumann entropy, as shown in Fig. 4.1 (b). This analysis aims to identify any enhancements in the rate of dynamical entropy associated with DQPTs. The results are shown in Fig. 4.2. We see that compared with the rate function the rate of change of dynamic entropy remains constant, apart from an initial peak that corresponds to the start of the process. Unlike Refs. [95], where they compared critical points of DQPT and entanglement entropy rate or [240], where they compared Wehrl entropy rate with DQPT we could not identify an enhancement in entropy or rate of dynamic entropy. In appendix C-II we have utilized another model and compared the rate function with rate of change of entanglement entropy. The results show no enhancement of the entropy rate near the critical points of rate function. This underlines the universality of the behavior in quantum helical systems.

Next in Fig. 4.3 we looked at the magnetization of the system and its dynamics due to the quenches. The dynamical magnetization followed by a quench to ferromagnet stays unchanged Fig. 4.3 (a). The initial state of the system was established in a skyrmionic phase with a magnetic field of $B = 0.85D$, and the DMI term D was subsequently turned off. The dynamics of the ground state were monitored over a prolonged period and the expectation value of the spin projection along the z-axis ($\langle S_z \rangle$) was evaluated. During this transition, the $\langle S_z \rangle$ remained constant. The dashed black line shows the equilibrium magnetization of the ferromagnetic state, as shown in Ref. [238]. Contrary to this observation when quenched from skymion to helical phase the magnetization value gradually shifts and makes small oscillating pattern about the expectation value of the corresponding equilibrium state Fig. 4.3 (b). Here also we start the system at skyrmion phase with $B = 0.85D$. At time $t = 0.0$ magnetic field B is turned off. Then the ground state is evolved and $\langle S_z \rangle$ is

measured. In contrast to the transition to the ferromagnetic phase, the $\langle S_z \rangle$ was found to exhibit oscillations around the equilibrium value of the helical phase. This contrast is mainly because, in the Hamiltonian Eq. B.1 when $D = 0$ the total magnetization operator commutes with the Hamiltonian, conserving the magnetization. For comparison, the black dashed line shows the equilibrium magnetization of the helical state to which the quench is performed, as shown in Ref. [238].

We looked at the evolution of the scalar chirality as well, after the two cases of quenches that we considered. In Fig. 4.4 (a) we see the observed C_ψ vs t graph when quenched from a skyrmion to ferromagnetic phase. In Fig. 4.4 (b) we have plotted C_ψ vs t for skyrmion to helical quench. In both cases, we see that the scalar chirality tends to fall to the equilibrium scalar value. It shows prominent oscillations compared with other quantities that we observed. The black dashed lines in Figs. 4.4 (a) and (b) represents the corresponding scalar chirality value of the equilibrium ground state of the quenched Hamiltonian, as shown in Ref. [238].

Next, we investigated topological entropy, which is considered a signature of topological states. The dynamical behavior for the two quenches are showcased in Fig. 4.5 (a) for skyrmion to ferromagnetic and in Fig. 4.5 (b) for skyrmion to helical quench. In the former case, we see that the expectation value falls in magnitude but not enough to reach its equilibrium value which is zero. In the latter case, the dynamical expectation value tends to progress towards the corresponding equilibrium expectation value. The black dashed lines show the corresponding equilibrium topological entropy of the ground state of the quenched Hamiltonian, as shown in Ref. [232]. We do not see a dependence of DQPT on the dynamics of the topological entropy.

4.4 Conclusions

This study explores entanglement entropy, a fundamental property of quantum many-body systems, in the context of dynamical quantum phase transitions (DQPTs) within a quantum helical system exhibiting topological order. By examining the interplay between entanglement dynamics, topology, and nonequilibrium phase transitions, we aim to deepen our understanding of quantum critical phenomena.

Our findings indicate that in the case of a quantum skyrmion, the occurrence of a DQPT does not correspond to a significant enhancement in entanglement entropy. We observe that entanglement entropy initially increases when the system undergoes a quench from a topological phase to either a helical or ferromagnetic phase. However, beyond this initial rise, it stabilizes, oscillating around a saturation value.

Notably, this increase in entanglement entropy occurs regardless of whether a DQPT is present, suggesting that its primary driver in this system is the nonequilibrium nature of the quench process rather than the critical transition itself. Moreover, the rate of change of entanglement entropy and scalar chirality do not exhibit significant anomalies around DQPT critical points, indicating that these quantities may not serve as reliable indicators of DQPT in this system.

In contrast, topological entanglement entropy—an intrinsic measure of topological order—and magnetization display distinct behavior near DQPT, making them more sensitive to the quenches. This disparity in the responses of different observables suggests that the system exhibits intricate dynamical features that cannot be fully captured by entanglement measures alone.

Further investigation is needed to understand why these quantities behave differently with respect to the presence/absence of DQPT.

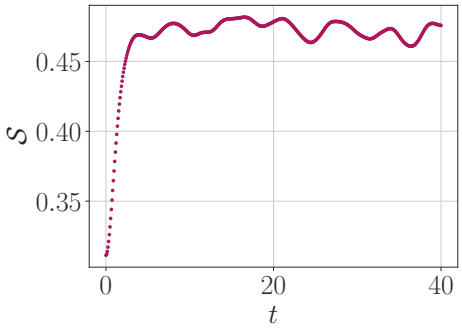

(a)

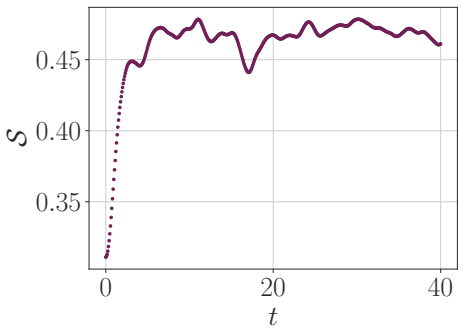

(b)

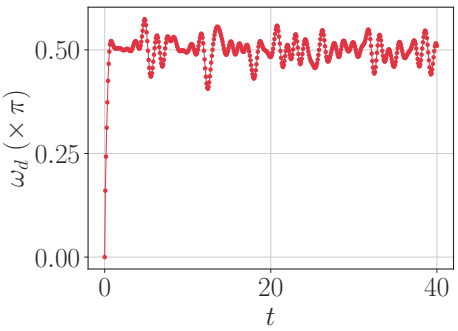

(c)

Fig. 4.1 a) The von Neumann entropy of a quenched state from skyrmionic phase to ferromagnetic phase was investigated. The ground state of the system was prepared in the skyrmionic phase with a magnetic field strength of $0.85D$. Dzyaloshinskii-Moriya Interaction (DMI) term was then turned off, and the ground state was allowed to evolve under quench. b) The von Neumann entropy entropy of quenched state from skyrmionic phase to helical phase. The system was initially prepared in the skyrmionic phase with a magnetic field strength of $0.85D$. At time $t = 0.0$, the magnetic field B was turned off, and the ground state was allowed to evolve. c) Wootters' distance, ω_d, between states undergoing quenches from skyrmionic to ferromagnetic/helical phase. In all cases, values of $D = 1,;J_1 = -0.5D$, and $J2 = 0.1D$.

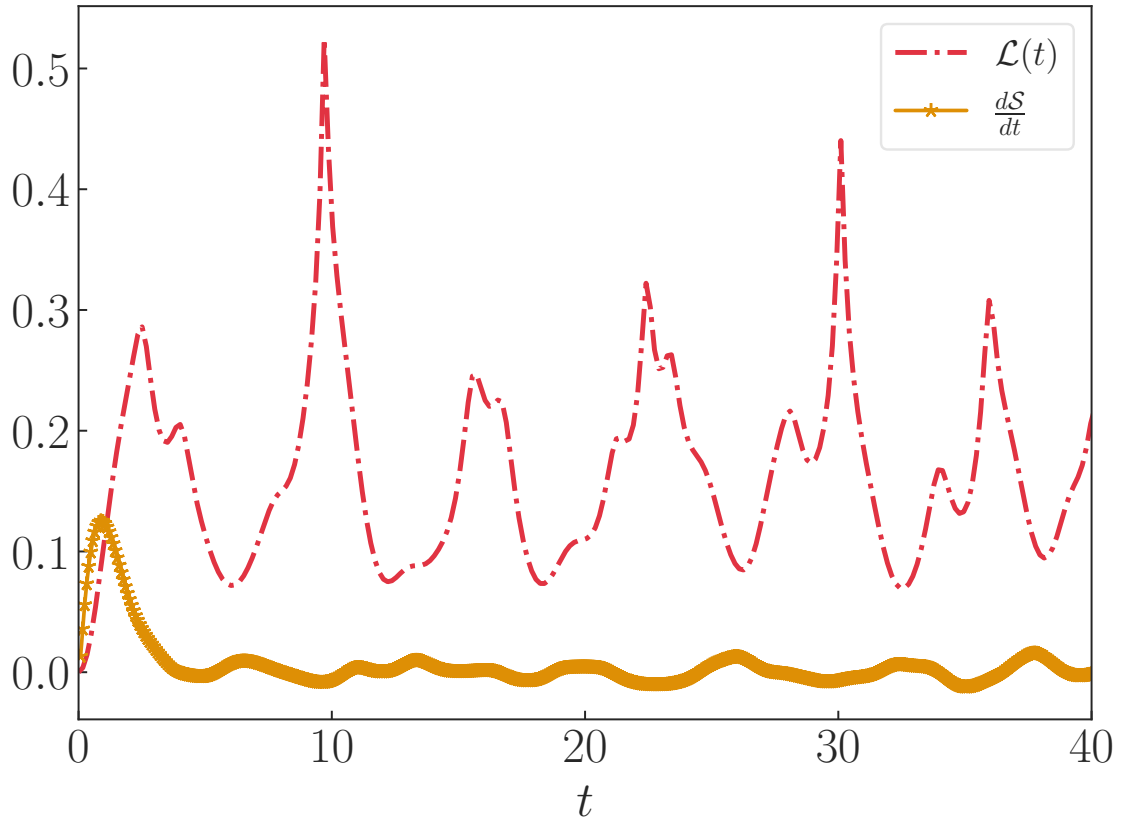

Fig. 4.2 The rate of change of entanglement entropy and the rate function of the return probability are compared for a system of 19 spins.

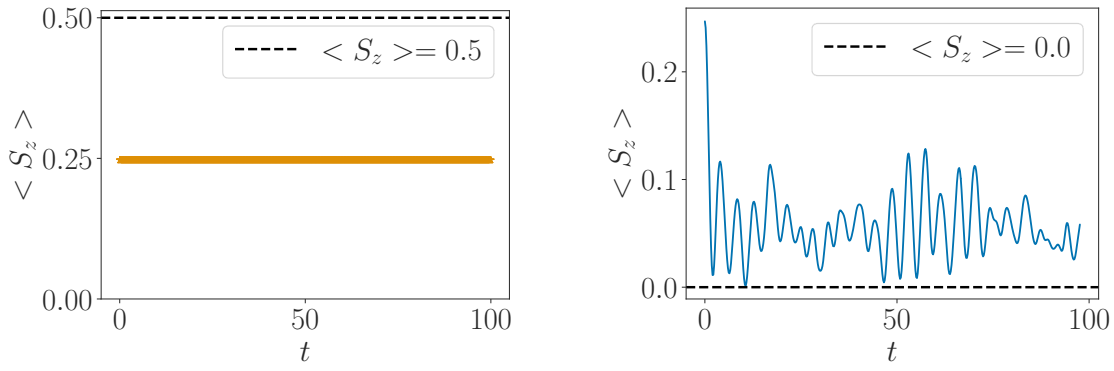

(a) (b)

Fig. 4.3 a) Magnetization of a quenched state from a skyrmion to a ferromagnetic phase. b) *Magnetization of quenched state from skyrmion to helical phase*. In all the cases $D = 1$, $J_1 = -0.5D$, and $J2 = 0.1D$. Dashed lines in the plots show the equilibrium values of the corresponding quenched state.

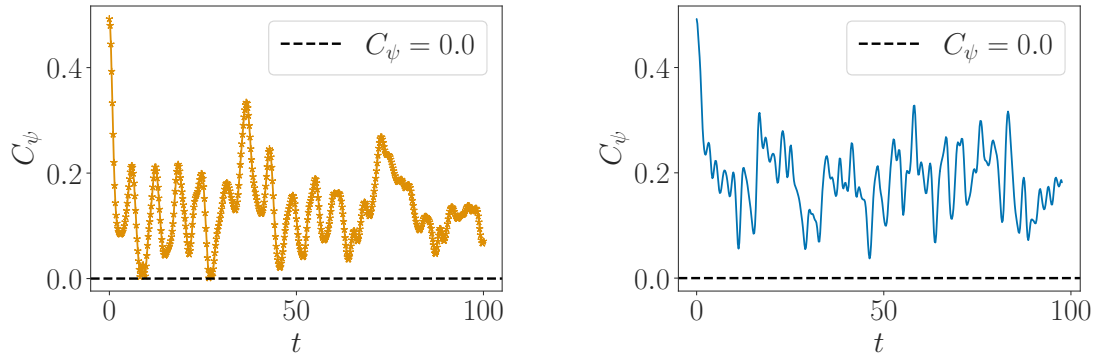

(a) (b)

Fig. 4.4 a) *Scalar chirality of quenched state from skyrmion to ferromagnetic phase*. We made the ground state of the system to be in skyrmionic phase with $B = .85D$, then we turned off the DMI term D, and the ground state evolved under the quench. C_ψ is observed for a long time duration. Here we see that the expectation value oscillates around the equilibrium value of the helical phase. b) *Chirality of quenched state from skyrmion to helical phase*. Here also we start the system at skyrmion phase with $B = 0.85D$. At time $t = 0.0$ magnetic field B is turned off. Then the ground state is evolved and C_ψ is measured. C_ψ decays to the equilibrium value and oscillates slightly. In all the cases $D = 1$, $J_1 = -0.5D$, and $J2 = 0.1D$.

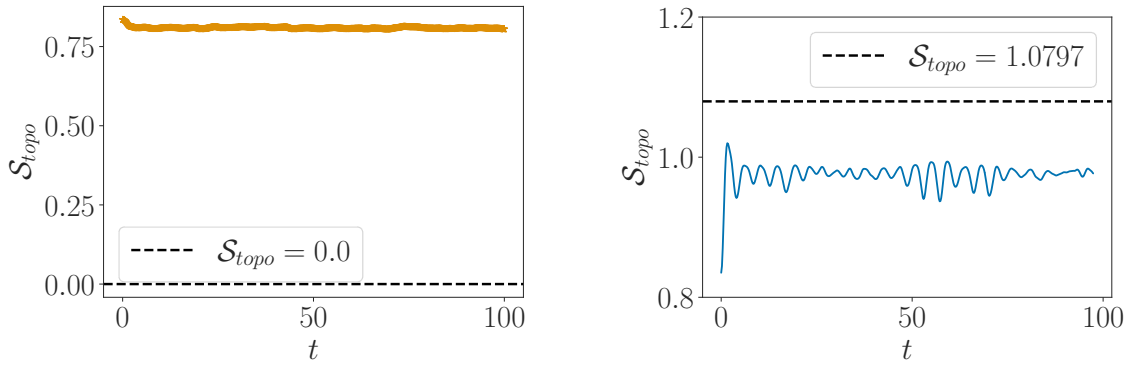

(a) (b)

Fig. 4.5 a) *Topological entanglement entropy of quenched state from skyrmion to ferromagnetic phase*. We made the ground state of the system to be in the skyrmionic phase with $B = 0.85D$, then we turned off the DMI term D and let the ground state evolve under the quench. $\mathscr{S}_{topo}$ is observed for a long time duration. b) *Topological entropy of quenched state from skyrmion to helical phase*. Here also we start the system at skyrmion phase with $B = 0.85D$. At time $t = 0.0$ magnetic field B is turned off. Then the ground state is evolved and $\mathscr{S}_{topo}$ is measured. Unlike the quench to a ferromagnetic phase when quenched to a helical phase the topological entropy shows an oscillating pattern. In all the cases $D = 1$, $J_1 = -0.5D$, and $J2 = 0.1D$.